

Refined analysis on the parton distribution functions of the proton

X G Wang, A W Thomas

CSSM and ARC Centre of Excellence for Particle Physics at the Terascale,
Department of Physics, University of Adelaide SA 5005 Australia

E-mail: xuan-gong.wang@adelaide.edu.au, anthony.thomas@adelaide.edu.au

Abstract. We explore the application of a two-component model of proton structure functions in the analysis of deep-inelastic scattering (DIS) data at low Q^2 and small x . This model incorporates both vector meson dominance and the correct photo-production limit. The CJ15 parameterization is applied to the QCD component, in order to take into account effects of order $1/Q^2$ effects, such as target mass corrections and higher twist contributions. The parameters of the leading twist parton distribution functions and higher twist coefficient functions are determined by fitting deep inelastic scattering data. The second moments of the parton distribution functions are extracted and compared with other global fits and lattice determinations.

Keywords: Parton distribution functions, vector meson dominance, deep inelastic scattering

Submitted to: *J. Phys. G: Nucl. Part. Phys.*

1. Introduction

Understanding the inner structure of the nucleon remains one of the most challenging tasks in modern particle and nuclear physics. It is of special interest how the nucleon's momentum and spin are divided among quarks and gluons. Within quantum chromodynamics (QCD), this information can be accessed through parton distribution functions (PDFs). Specifically, the second moments of unpolarised PDFs are interpreted as the momentum fractions carried by partons.

There are mainly two approaches to studying PDFs of nucleons. First, the PDFs are determined from global fits to the world data on deep inelastic scattering (DIS) and related hard scattering processes [1, 2]. One usually starts from a parametrisation of the initial PDFs at somehow low scale, and then evolves to high Q^2 region using the DGLAP equations. Nowadays, with improvement in the precision and kinematic range of the experimental measurements from Jefferson Lab, HERA, RHIC, the Tevatron and the LHC, global fits have covered data over a broad range of Bjorken x and four-momentum transfer Q^2 [3, 4, 5].

The second method is lattice QCD. Early lattice simulations were limited to the nucleon matrix elements of leading-twist (LT) local operators, which correspond to the low moments of PDFs. Recent approaches to determining the x -dependent PDFs have been proposed, either in terms of quasi-PDFs [6, 7], or in terms of pseudo-PDFs [8, 9].

Efforts have been made to establish connections between these two approaches [10]. The results from global fits are useful in validating current and future lattice simulations. On the other hand, the lattice results could be used to reduce the uncertainties in current global analysis of PDFs.

However, a surprising difference between global fits and lattice calculations of the moment of unpolarized flavor-singlet PDFs was observed recently. At $Q^2 = 4 \text{ GeV}^2$, the global fit determinations give

$$\begin{aligned} \langle x \rangle_{u^+}^{\text{exp}} &= 0.352(12), \quad \langle x \rangle_{d^+}^{\text{exp}} = 0.192(6), \\ \langle x \rangle_{s^+}^{\text{exp}} &= 0.037(3), \quad \langle x \rangle_g^{\text{exp}} = 0.411(8), \end{aligned} \quad (1)$$

while the latest lattice simulations from ETMC17 gave significantly larger results, albeit with large uncertainties [11],

$$\begin{aligned} \langle x \rangle_{u^+}^{\text{lat}} &= 0.453(75), \quad \langle x \rangle_{d^+}^{\text{lat}} = 0.259(74), \\ \langle x \rangle_{s^+}^{\text{lat}} &= 0.092(41), \quad \langle x \rangle_g^{\text{lat}} = 0.267(35). \end{aligned} \quad (2)$$

As discussed in Ref. [10], it may be that this discrepancy would be removed by taking into account the renormalisation properly and imposing momentum sum rule in lattice calculations.

However, the discrepancy may also originate from the global-fit side. The experimental results include both short and long distance physics. This can be seen from the flavor-singlet light-cone correlation functions which are obtained by Fourier transforming the empirical PDFs in momentum space. The resulting distributions extend over large distances [12], reflecting primarily the partonic structure of the photon

in the very small x region, i.e., the virtual photon fluctuates into a $q\bar{q}$ pair [13]. This effect is usually saturated by the vector meson dominance (VMD) model.

On the other hand, when $Q^2 \rightarrow 0$, F_2 must vanish linearly with Q^2 in order to give a finite photo-production cross section. Such behavior cannot be generated by DGLAP evolution to low- Q^2 .

A two-component model to separate perturbative and non-perturbative contributions to the proton structure function was first proposed by Badelek and Kwiecinski [14, 15]. Incorporating the vanishing of F_2 in the $Q^2 = 0$ limit as well as the scaling behaviour at large Q^2 , the proton structure function is written as [14, 15, 16]

$$F_2(x, Q^2) = F_2(VMD) + \frac{Q^2}{Q^2 + Q_0^2} F_2^{\text{QCD}}(\bar{x}, Q^2 + Q_0^2), \quad (3)$$

where

$$\bar{x} = \frac{Q^2 + Q_0^2}{s + Q^2 + Q_0^2 - M^2} = x \frac{Q^2 + Q_0^2}{Q^2 + xQ_0^2}. \quad (4)$$

Q_0 should be larger than the mass of the heaviest vector meson included in the VMD contribution, but smaller than the mass of the lightest vector meson not included. While some analysis gave relatively small values of Q_0^2 by treating it as free parameter [17, 18], it is reasonable to choose Q_0^2 in the range $1.0 \sim 1.5 \text{ GeV}^2$ [16].

Various parametrizations of PDFs in the literature may be used for the QCD component, F_2^{QCD} . One of our aims is to make a comparison between the moments of the PDFs extracted from this two-component model and the lattice simulations. Here we take the CJ15 formalism [5] and redetermine some of the parameters by fitting data on the proton deep inelastic scattering structure functions. The second moments of the leading twist PDFs are also derived.

2. Vector Meson Dominance

The vector meson dominance term has the form

$$F_2(VMD) = \frac{Q^2}{\pi} \sum_V \frac{M_V^4 \sigma_{VN}}{f_V^2 (Q^2 + M_V^2)^2}, \quad (5)$$

where $V = \rho^0, \omega$ and ϕ and the photon-vector-meson coupling constants are

$$\frac{f_V^2}{4\pi} = \frac{\alpha^2 M_V}{3\Gamma_{V \rightarrow e^+e^-}}, \quad (6)$$

equal to 2.28, 26.14, and 14.91 for ρ^0 , ω and ϕ , respectively. For the vector meson-proton cross sections, we take

$$\begin{aligned} \sigma_{\rho p} &= \sigma_{\omega p} = \frac{1}{2} [\sigma(\pi^+ p) + \sigma(\pi^- p)], \\ \sigma_{\phi p} &= \sigma(K^+ p) + \sigma(K^- p) - \frac{1}{2} [\sigma(\pi^+ p) + \sigma(\pi^- p)], \end{aligned} \quad (7)$$

together with the parametrisation form [19]

$$\begin{aligned} \sigma_{\rho p} &= \sigma_{\omega p} = 13.63 s^\epsilon + 31.79 s^{-\eta}, \\ \sigma_{\phi p} &= 10.01 s^\epsilon + 2.72 s^{-\eta}, \end{aligned} \quad (8)$$

where $\epsilon = 0.08$ and $\eta = 0.45$ are taken from Regge theory and the resulting cross sections are in unit of mb.

The VMD contribution is a higher twist (HT) effect because of the vector meson propagators, so that it is negligible for large Q^2 . Moreover, it is only relevant when the lifetime of the hadronic fluctuation of photon is larger than the interaction time $\tau_{\text{int}} \sim R$ [20],

$$\tau \sim \frac{1}{\Delta E} \geq R, \quad (9)$$

where R is the electromagnetic radius of the proton and in the target reference frame

$$\Delta E = \frac{M_V^2 + Q^2}{Q^2} \cdot M_N x. \quad (10)$$

This constraint usually implies that the VMD contributions are important in region where Bjorken x is small, $x \leq 0.1$. In order to incorporate this effect, the standard VMD component was modified by introducing a form factor in [18],

$$F_2(VMD) = \frac{Q^2}{\pi} \sum_V \frac{M_V^4 \sigma_{VN}}{f_V^2 (Q^2 + M_V^2)^2} \Omega(x, Q^2), \quad (11)$$

where a Gaussian form was preferred by the best fit,

$$\Omega(x, Q^2) = \exp(-(\Delta E/\lambda_G)^2), \quad (12)$$

with $\lambda_G = 0.50 \text{ GeV}$. However, with this choice, the VMD contributions survive up to relatively large $x \sim 0.5$. In fact, the proton radius provides a natural characteristic scale and therefore in our analysis we choose instead

$$\lambda_G = 1/R = 0.25 \text{ GeV}. \quad (13)$$

A possible non-diagonal term corresponding to the $\rho^0 p \rightarrow \omega^0 p$ transition was found to be negligibly small [21], while the non-diagonal $\omega p \rightarrow \phi p$ and $\rho p \rightarrow \phi p$ transitions are neglected on the basis of the Zweig rule.

3. The QCD component

The standard partonic parametrization, together with $1/Q^2$ corrections such as target mass correction (TMC) and QCD induced higher twist effects [5], could be applied to the QCD component of the proton structure function,

$$F_2^{\text{QCD}}(x, Q^2) = F_2^{\text{LT}}(x, Q^2) \left(1 + \frac{C_{\text{HT}}(x)}{Q^2} \right), \quad (14)$$

where F_2^{LT} denotes the leading-twist structure function, including TMC effects,

$$\begin{aligned} F_2^{\text{LT}}(x, Q^2) &= \frac{(1+\rho)^2}{4\rho^3} F_2^{(0)}(\xi, Q^2) + \frac{3x(\rho^2-1)}{2\rho^4} \int_{\xi}^1 du \\ &\times \left[1 + \frac{\rho^2-1}{2x\rho}(u-\xi) \right] \frac{F_2^{(0)}(u, Q^2)}{u^2}, \end{aligned} \quad (15)$$

with $F_2^{(0)}$ being the structure function in the $M^2/Q^2 \rightarrow 0$ limit, and the modified scaling variable

$$\xi = \frac{2x}{1+\rho}, \quad \rho^2 = 1 + \frac{4x^2 M^2}{Q^2}. \quad (16)$$

In order to allow flexibility in the shape of the higher-twist contribution, following the discussions in [22], the higher-twist coefficient function is parametrized by a polynomial function as

$$C_{\text{HT}}(x) = h_0 x^{h_1} (1 + h_2 x). \quad (17)$$

The initial PDFs are taken from the CJ15 parametrisation at $m_c^2 = 1.69 \text{ GeV}^2$,

$$xf(x, Q^2) = a_0 x^{a_1} (1-x)^{a_2} (1 + a_3 \sqrt{x} + a_4 x), \quad (18)$$

for the valence $u_v = u - \bar{u}$ and $d_v = d - \bar{d}$, the light antiquark sea $\bar{u} + \bar{d}$, and the gluon distribution g . In [5], the d_v distribution was modified by adding a small admixture of the valence u -quark PDF with two additional parameters b and c ,

$$d_v \rightarrow a_0^{d_v} \left(\frac{d_v}{a_0^{d_v}} + bx^c u_v \right). \quad (19)$$

In the $x \rightarrow 1$ limit, it leads to a finite, nonzero value of the ratio

$$\frac{d_v}{u_v} \rightarrow a_0^{d_v} b = 8.89 \times 10^{-2}. \quad (20)$$

The functional form of \bar{d}/\bar{u} at the input scale is taken to be

$$\frac{\bar{d}}{\bar{u}} = a_0 x^{a_1} (1-x)^{a_2} + 1 + a_3 x (1-x)^{a_4}. \quad (21)$$

The strange quark distribution is related to the light quark sea through a fixed ratio

$$\kappa = \frac{s + \bar{s}}{\bar{u} + \bar{d}}, \quad (22)$$

which was set to be 0.4 in [5]. The sensitivity of the fit to this parameter was examined by varying κ in the range $0.3 \sim 0.5$.

4. Results

In contrast to global fits, the present DIS only analysis is subject to some limitations. In particular, the present work should be regarded as exploratory, aimed at investigating whether a full scale search based on this approach would be justified. Bearing in mind the limited data set used here we find it necessary to constrain some parameters. First of all, the strongest constraint on \bar{d}/\bar{u} comes from the Drell-Yan process, so we fix the parameters of \bar{d}/\bar{u} at CJ15 values. Second, since the proton structure function is less sensitive to the d quark distribution, we fix the d/u ratio from the CJ15 analysis. Then, the valence d quark distribution can be expressed as

$$d_v(x, Q^2) = \left(\frac{d}{u} \right)_{\text{CJ15}} u(x, Q^2) - \left(\frac{\bar{d}}{\bar{u}} \right)_{\text{CJ15}} \bar{u}(x, Q^2). \quad (23)$$

Table 1. The fitted LT parameter values for u_v , $\bar{d} + \bar{u}$, and g PDFs from NLO analysis, and the HT parameters for the coefficient function, with $Q_0^2 = 1.0 \text{ GeV}^2$ and $\kappa = 0.4$. The $\chi_{d.o.f}^2 = 116/(129 - 9) = 0.97$.

LT	u_v	$\bar{d} + \bar{u}$	g	HT	
a_0	2.4525	0.11871	23.617	h_0	-1.2244 ± 0.37427
a_1	0.61931 ± 0.0048790	-0.20943 ± 0.055740	0.36755 ± 0.035769	h_1	0.59992 ± 0.12744
a_2	3.6177 ± 0.032649	8.3286	6.4812	h_2	-9.5558 ± 2.7204
a_3	0	0	-3.3064		
a_4	3.5445 ± 0.13391	26.215 ± 7.5988	3.1721		

Table 2. The fitted LT parameter values for u_v , $\bar{d} + \bar{u}$, and g PDFs from NLO analysis, and the HT parameters for the coefficient function, with $Q_0^2 = 1.5 \text{ GeV}^2$ and $\kappa = 0.4$. The $\chi_{d.o.f}^2 = 138/(129 - 9) = 1.15$.

LT	u_v	$\bar{d} + \bar{u}$	g	HT	
a_0	1.7831	0.29270	16.532	h_0	-0.87901 ± 0.37427
a_1	0.54552 ± 0.010214	-0.049054 ± 0.058255	0.25347 ± 0.030693	h_1	0.81821 ± 0.065805
a_2	3.6998 ± 0.030355	8.3286	6.4812	h_2	-23.867 ± 5.9689
a_3	0	0	-3.3064		
a_4	5.3979 ± 0.19655	14.771 ± 4.6105	3.1721		

Moreover, we also fix a_2 , a_3 , and a_4 of xg , as the structure function F_2 is insensitive to the large x behaviour of gluon distribution.

The parameters a_0 for xu_v , $x(\bar{d} + \bar{u})$ and xg are constrained by number and momentum sum rules and are therefore not free parameters. There remain 9 free parameters, which will be determined by fitting the DIS data of the proton structure function. The experimental data are taken from BCDMS [23], SLAC [24], NMC [25], E665 [26]. While the CJ15 analysis fits data above $x_{\min} = 5 \times 10^{-3}$, we also include H1 data in the very small x region [27], down to 1.3×10^{-4} . We choose data points of several Q^2 bins around 5, 10, 20, 25 and 50 GeV^2 , which are sufficient to fix the LT PDF parameters as well as the HT coefficient function. Statistical and systematic errors are added in quadrature.

The LT structure function in (14), F_2^{LT} , is derived by NLO QCD evolution using APFEL program [28], including target mass corrections. By fixing $\kappa = 0.4$, the parameters of the initial PDFs and the HT coefficient function are given in Tables 1 and 2, corresponding to $Q_0^2 = 1.0 \text{ GeV}^2$ and $Q_0^2 = 1.5 \text{ GeV}^2$, respectively. Compared with the CJ15 results, the parameters a_0 and a_1 for the gluon distribution are much smaller, while the HT coefficient function is enhanced in the large x region, because of the larger value of h_2 .

In the case of $Q_0^2 = 1.0 \text{ GeV}^2$ and $\kappa = 0.4$, the fitted structure functions are shown in Fig. 1, with $\chi_{d.o.f}^2 = 116/(129 - 9) = 0.97$. For $Q^2 = 4 \text{ GeV}^2$, we also show in Fig. 2 the individual contribution from each component to the total structure function.

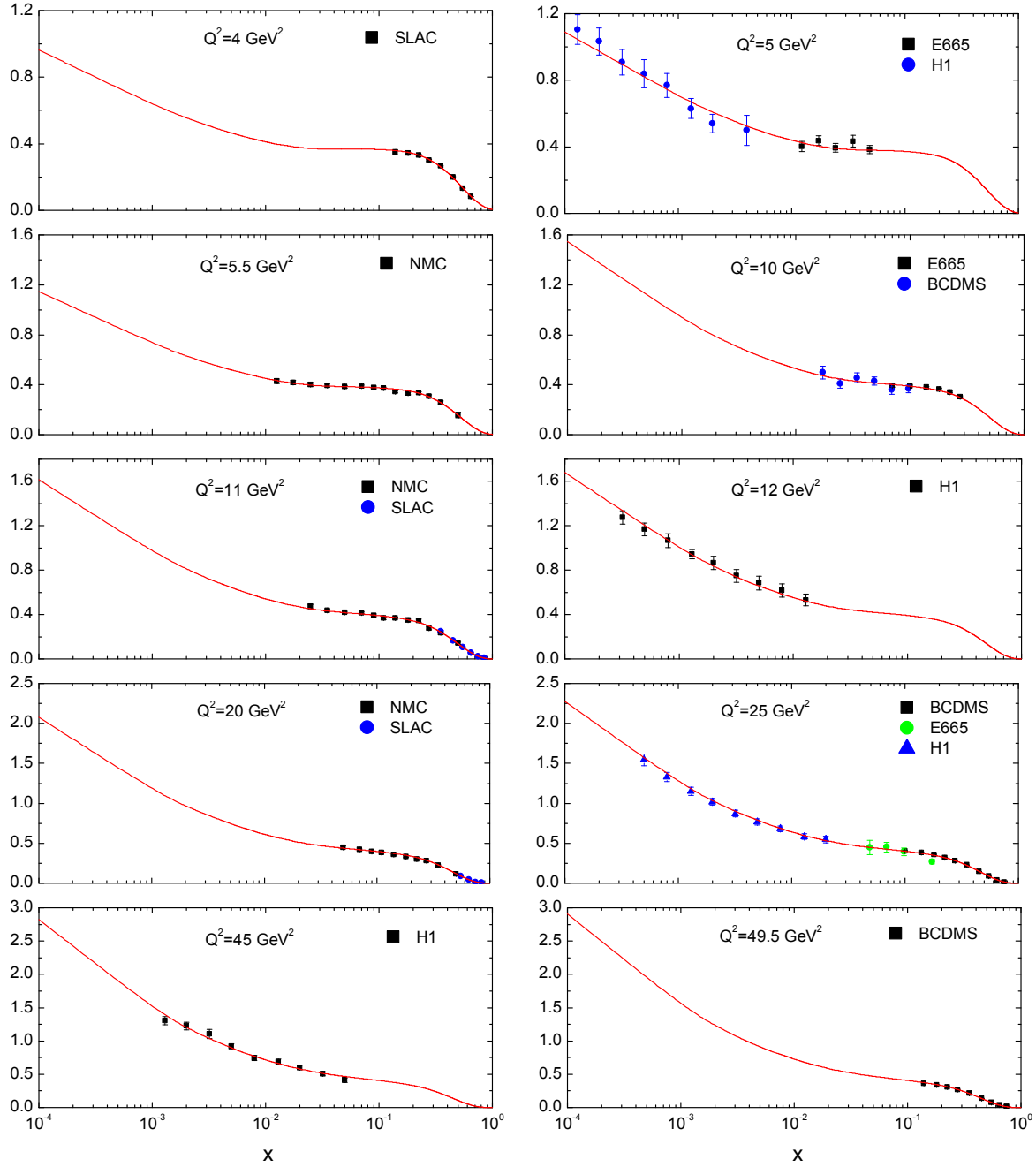


Figure 1. The fit results of the proton structure functions with $Q_0^2 = 1.0 \text{ GeV}^2$ and $\kappa = 0.4$.

Although negligible for large Q^2 , the VMD contribution accounts for (10 – 20)% of the total F_2 at $x \leq 0.1$. The significant enhancement in F_2^{QCD} compared to F_2^{LT} when $x > 0.1$ indicates large HT effect, which is associated with the parameter h_2 .

The LT PDFs at $Q^2 = 4 \text{ GeV}^2$ are displayed in Fig. 3 and compared with the CJ15 results. The valence quark distributions xu_v and xd_v are almost unchanged. In addition, the d_v given in (23) results in $d_v/u_v \rightarrow 8.80 \times 10^{-2}$ as $x \rightarrow 1$, which is consistent with

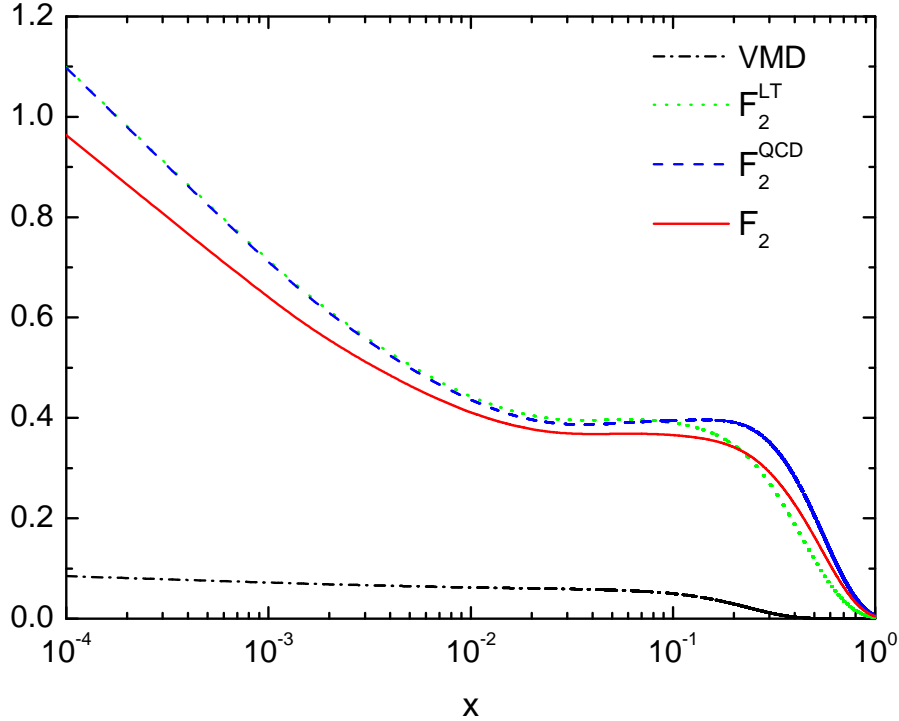


Figure 2. Individual contribution from each component to the proton structure function at $Q^2 = 4 \text{ GeV}^2$, with $Q_0^2 = 1.0 \text{ GeV}^2$ and $\kappa = 0.4$.

the CJ15 value in (20). However, there is a noticeable difference for $x(\bar{u} + \bar{d})$ and a large difference for the distribution xg . Our analysis tends to result in a smaller sea quark distribution and a significantly larger gluon distribution in the small x region. While in the range $0.05 \leq x \leq 0.5$, we find a sizeable increase in $x(\bar{u} + \bar{d})$ and small decrease in xg , in comparison with the CJ15 PDFs.

We also repeat the same fit procedure with different values of Q_0^2 and κ . The corresponding second moments of the LT PDFs at $Q^2 = 4 \text{ GeV}^2$ are summarized in Table 3. Within the limits of Q_0^2 and κ , the momentum fraction carried by gluons is a few percent smaller than the previous global-fit determination.

5. Conclusion

In this paper, we argue that a two-component model of nucleon structure functions incorporating the VMD contribution as well as the correct photo-production limit is more appropriate when describing DIS data in the low Q^2 and small x region. The QCD component is expressed in terms of the CJ15 parametrization. The parameters of the LT PDFs and the HT coefficient function were redetermined by fitting inclusive deep-inelastic scattering data for the proton. Our analysis shows that the application of

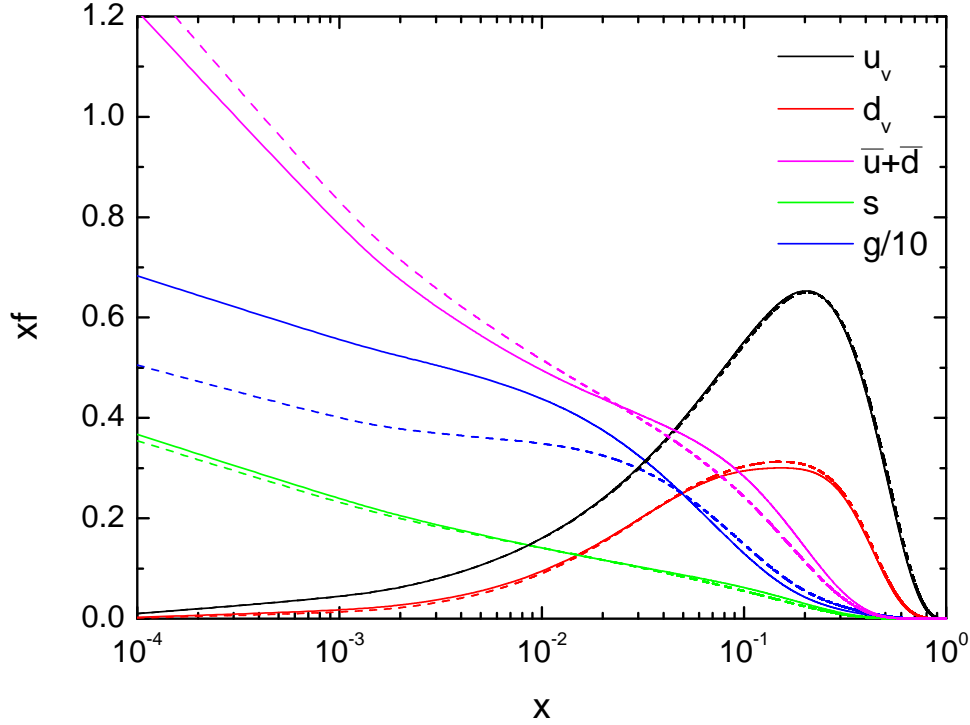


Figure 3. Parton distribution functions at $Q^2 = 4 \text{ GeV}^2$. The solid lines are our fit results, while the dashed lines are the corresponding PDFs from CJ15 results.

Table 3. The second moments of LT PDFs at $Q^2 = 4 \text{ GeV}^2$.

$Q_0^2(\text{GeV}^2)$	κ	$\langle x \rangle_{u+}$	$\langle x \rangle_{d+}$	$\langle x \rangle_{s+}$	$\langle x \rangle_g$
1.0	0.3	0.3552	0.2049	0.0283	0.4033
	0.4	0.3543	0.2039	0.0344	0.3993
	0.5	0.3538	0.2027	0.0397	0.3958
1.5	0.3	0.3572	0.2108	0.0312	0.3920
	0.4	0.3554	0.2095	0.0386	0.3879
	0.5	0.3542	0.2084	0.0459	0.3831
CJ15 [5]	0.4	0.3488	0.1965	0.0311	0.4152

the two component model mainly affects the $x(\bar{u} + \bar{d})$ and xg distributions in the small and moderate x regions. The second moments of the PDFs were also derived, with the results suggesting only small increases in the moments of the quark distributions and correspondingly a smaller value of the momentum fraction carried by gluons. Far from explaining the significant discrepancy between the global-fit determinations and the lattice results, the present analysis confirms the former.

Further improvements can be made by embedding this two-component model of

structure functions into a global-fit program, in which one can remove the constraints used in the present work and determine all of the parameters more precisely.

Acknowledgments

We would like to thank Wally Melnitchouk for helpful discussions and comments . This work was supported by the Australian Research Council through Discovery Projects DP151103101 and DP180100497.

References

- [1] Martin A D, Roberts R G, Stirling W G and Thorne R S 1998 Parton distributions: a new global analysis *Eur. Phys. J. C* **4** 463
- [2] Glück M, Reya E and Vogt A 1998 Dynamical parton distributions revisited *Eur. Phys. J. C* **5** 461
- [3] Harland-Lang L A, Martin A D, Motylinski P and Thorne R S 2015 Parton distributions in the LHC era: MMHT 2014 PDFs *Eur. Phys. J. C* **75** 204
- [4] Ball R D *et al* (NNPDF Collaboration) 2015 Parton distributions for the LHC Run II *J. High Energy Phys.* JHEP04(2015)040
- [5] Accardi A, Brady L T, Melnitchouk W, Owens J F and Sato N 2016 Constraints on large- x parton distributions from new weak boson production and deep-inelastic scattering data *Phys. Rev. D* **93** 114017
- [6] Ji X 2013 Parton physics on a Euclidean lattice *Phys. Rev. Lett.* **110** 262002
- [7] Lin H W, Chen J W, Cohen S D and Ji X 2015 Flavor structure of the nucleon sea from lattice QCD *Phys. Rev. D* **91** 054510
- [8] Radyushkin A V 2017 Quasi-parton distribution functions, momentum distributions, and pseudo-parton distribution functions *Phys. Rev. D* **96** 034025
- [9] Orginos K, Radyushkin A, Karpie J and Zafeiropoulos S 2017 Lattice QCD exploration of parton pseudo-distribution functions *Phys. Rev. D* **96** 094503
- [10] Lin H W *et al* 2018 Parton distributions and lattice QCD calculations: A community white paper *Prog. Part. Nucl. Phys.* **100** 107
- [11] Alexandrou C *et al* 2017 Nucleon spin and momentum decomposition using lattice QCD simulations *Phys. Rev. Lett.* **119** 142002
- [12] Braun V, Gornicki P and Mankiewicz L 1995 Ioffe-time distributions instead of parton momentum distributions in description of deep inelastic scattering *Phys. Rev. D* **51** 6036
- [13] Vanttinen M, Piller G, Mankiewicz L, Weise W and Eskola K J 1998 Nuclear quark and gluon distributions in coordinate space *Eur. Phys. J. A* **3** 351
- [14] Kwiecinski J and Badelek B 1989 Analysis of the electroproduction structure functions in the low Q^2 region combining the vector meson dominance and the parton model with possible scaling violation *Z. Phys. C* **43** 251
- [15] Badelek B and Kwiecinski J 1992 Electroproduction structure function F_2 in the low Q^2 , low x region *Phys. Lett. B* **295** 263
- [16] Martin A D, Ryskin M G, Stasto A M 1999 The description of F_2 at low Q^2 *Eur. Phys. J. C* **7** 643
- [17] Adloff C *et al* (H1 Collaboration) 1997 A measurement of the proton structure function $F_2(x, Q^2)$ at low x and low Q^2 at HERA *Nucl. Phys. B* **497** 3
- [18] Szczurek A and Uleshchenko V 2000 Nonpartonic components in the nucleon structure functions at small Q^2 in a broad range of x *Eur. Phys. J. C* **12** 663
- [19] Donnachie A and Landshoff P V 1992 Total cross sections *Phys. Lett. B* **296** 227

- [20] Levy A 1997 The proton and photon, who is probing whom? *Phys. Lett. B* **404** 369
- [21] Kwiecinski J 1983 Linking total cross-sections for hard and soft processes through analyticity in Q^2 and sum rules *Phys. Lett. B* **120** 418
- [22] Accardi A, Christy M E, Keppel C E, Melnitchouk M, Monaghan P, Morfin J G, and Owens J F 2010 New parton distributions from large- x and low- Q^2 data *Phys. Rev. D* **81** 034016
- [23] Benvenuti A C *et al* (BCDMS Collaboration) 1989 A high statistics measurement of the proton structure functions $F_2(x, Q^2)$ and R from deep inelastic muon scattering at high Q^2 *Phys. Lett. B* **223** 485
- [24] Whitlow L W, Riordan E M, Dasu S, Rock S and Bodek A 1992 Precise measurements of the proton and deuteron structure functions from a global analysis of the SLAC deep electron scattering cross-sections *Phys. Lett. B* **282** 475
- [25] Arneodo M *et al* (New Muon Collaboration) 1996 Measurement of the proton and deuteron structure functions, F_2^p and F_2^d , and of the ratio σ_L/σ_T *Nucl. Phys. B* **483** 3
- [26] Adams M R *et al* (E665 Collaboration) 1996 Proton and deuteron structure functions in muon scattering at 470 GeV *Phys. Rev. D* **54** 3006
- [27] Aid S *et al* (H1 Collaboration) 1996 A measurement and QCD analysis of the proton structure function $F_2(x, Q^2)$ at HERA *Nucl. Phys. B* **470** 3
- [28] Bertone V, Carrazza S and Rojo J 2013 APFEL: A PDF evolution library with QED corrections *Comput. Phys. Commun.* **185** 1647